ACS OMEGA

http://pubs.acs.org/journal/acsodf

Article

Adsorption and Interaction of Bovine Serum Albumin and Pluronic P103 Triblock Copolymer on a Gold Electrode: Double-Layer Capacitance Measurements

Brenda Velasco-Rodriguez, J. Félix Soltero-Martínez, Luis Carlos Rosales-Rivera, Emma Rebeca Macías-Balleza, Gabriel Landázuri, and Erika Roxana Larios-Durán*

Cite This: *ACS Omega* 2020, 5, 17347−17355

Read Online

ACCESS | Metrics & More | Article Recommendations

ABSTRACT: The interactions of proteins and other molecules and their adsorption onto substrates is a fascinating topic that has been applied to surface technologies, biosensors, corrosion studies, biotechnologies, and other fields. The success of these applications requires a previous characterization using some analytical techniques that, ordinarily, are not electrochemical. This work proposes analyzing the variation of the double-layer capacitance obtained through impedance electrochemical spectroscopy as an alternative strategy to show evidence of the interactions between proteins and triblock copolymers. The proposal is supported through the study of the interaction and adsorption of bovine serum albumin (BSA) and a commercial triblock copolymer (P103) in phosphate buffer on a gold electrode. The double-layer capacitance and the apparent interface thickness vs polarization potential curves as well as the potential of zero charge for pure P103 (0.6 wt %, corresponding to 6 g L^{-1}), pure BSA (3 mg mL^{-1}), and P103-BSA solutions (0.6 wt % and 3 mg mL^{-1}, respectively) are sensitive enough to show not only the interaction and the adsorption of the species but also the polarization potential where these interactions are taking place. A qualitative and quantitative analysis concerning the double-layer capacitance behavior is given. The significance and impact of this work is also presented.

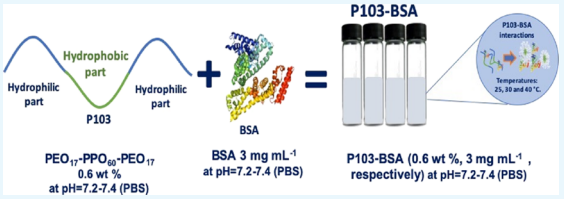

1. INTRODUCTION

The studies of interactions between proteins and metallic surfaces have had a positive impact on several biological, sensor, and applied biotechnological areas. For example, the study of protein adsorption on solid electrodes and its interaction with the surrounding medium is fundamental for the development of biosensors, medical implants, drug delivery systems, and switchable membranes, among others.[1−8] The adsorption of proteins on metallic surfaces depends on several physical and chemical aspects, such as protein concentration, pH, salt concentration, and ionic strength of the medium, surface charge of the substrate, isoelectric point, and electrostatic interaction at the protein/metal interface. Surface plasmon resonance (SPR) and ellipsometry are techniques that have been used to characterize protein adsorption on metallic surfaces and its interactions with the medium.[2,9] However, electrochemical techniques are adequate and highly sensitive for successfully evaluating not only the protein adsorption−desorption process on electrodes but also its possible denaturation at the surface. Techniques such as cyclic voltammetry (CV) and electrochemical impedance spectroscopy (EIS), along with electrochemical quartz crystal micro- and nanobalance and double-layer capacitance measurements, have been applied to the study of adsorption−desorption processes of proteins and emulsions on metallic electrodes.[9−16] According to the results, where bovine serum albumin (BSA) and human serum albumin have been the most studied proteins, the electrochemical techniques adequately demonstrate the adsorption−desorption process as a function of protein concentration, substrate charge, pH, and polarization potentials, allowing studies in the presence and absence of charge transfer. The versatility of the electrochemical techniques and the information acquired in the study of protein adsorption has increased their application, and thus, they are currently preferred over optical techniques for many researchers.[11]

Beyond the knowledge of the adsorption−desorption process of proteins, the scientific community is now interested in the interactions between proteins and other molecules, such as polymers and copolymers and biomolecules, such as polysaccharides. The main advances in this topic are focused on the interactions between triblock copolymers and proteins.[17−20] The interest in these kinds of interactions is due to the

Received: April 14, 2020
Accepted: June 25, 2020
Published: July 8, 2020

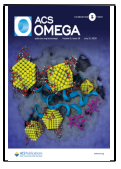

biocompatibility of the formed molecules, the acquired capacity to form micelles at low concentrations, and the increased facility to penetrate into cellular membranes, allowing drug deliveries[19,20] as well as possibilities in design for either biomaterials or biosensor surfaces.[21−24] The use of measurements such as conductivity, UV−Vis spectrophotometry, electron paramagnetic resonance and SPR has been commonly applied to characterize the interactions between proteins and triblock copolymers.[17−20] According to the literature, proteins and triblock copolymers interact either by electrostatic or hydrophobic effects. These effects modify the physical and chemical properties of both molecules. However, as reported in the literature,[25] although the ability of triblock copolymers to reduce protein adsorption is known, the detailed procedure involved in this phenomenon has not yet been clarified. Other interesting studies are those concerning polymers blends such as miscible homopolymer−copolymer pair.[26−29] In those studies, the miscibility in polymer−polymer systems is studied using calorimetric techniques and thermogravimetric analysis.

It should be noted that electrochemical studies concerning these interactions are scarcer and the most common imply the adsorption of the triblock copolymers or the proteins in an isolated manner.[9−16,24,25] The aim of this work is to study the triblock copolymer−protein−electrode interactions from the fundamental point of view of double-layer capacitance as calculated from EIS measurements and to obtain information about the behavior and apparent size of the interface formed by the adsorbed species on a gold disc electrode at different temperatures. The information obtained from this study is important in sensor and bio-surface design based on the detection of protein liberation or a reduced protein adsorption process in micelles. These processes can be sensed through the double-layer capacitance variations analytically measured by the abovementioned technique as a temperature function. Thus, the effect of the temperature could be evaluated avoiding the use of calorimeters.

The protein and copolymer studied are BSA and Pluronic P103, respectively. The Pluronic P103 triblock copolymer is formed with sequential blocks of poly(ethylene oxide) (PEO) and poly(propylene oxide) (PPO) in the form of PEO-PPO-PEO with the structure of $PEO_{17}PPO_{60}PEO_{17}$.[24,25] P103 was chosen due to its low toxicity, biodegradability, and tendency to form micelles in the range of 0.2−1 wt %. These properties make it an excellent vehicle for drug delivery.[20] On the other hand, BSA was selected because it is a model globular protein, and several sources of information concerning its adsorption on metallic surfaces are available.[18]

The study is focused on evaluating the double-layer capacitance as a function of the polarization potentials at 25, 30, and 40 °C for three systems: (i) pure P103 (0.6 wt %, corresponding to 6 g L^{-1}), (ii) pure BSA (3 mg mL^{-1}), and iii) mixtures of P103-BSA (0.6 wt % and 3 mg mL^{-1}, respectively). Well-defined changes in the double-layer capacitance values of each system are highly desirable to show evidence of modifications at the interface associated with the interaction of each one of the studied species. The interest of this study is focused on the polarization potential effect in the selective adsorption of both molecules as well as the interface thickness. However, particular emphasis is placed in the polarization range in which BSA protein is not denaturalized, which implies the absence of charge transfer and is a state ensured at the open-circuit potential. Furthermore, the potential of zero charge, obtained from the double-layer capacitance curves, is presented and analyzed through the classical electrochemical double-layer theory. Thus, the favorable polarization range where the adsorption and interaction of each studied species is shown. The calculation of the apparent interface thickness as a function of the polarization potential at constant temperature is also shown. For all the studied systems, cyclic voltammetry at a wide polarization potential range is presented to complement the information. In a further work, a thermodynamic analysis will be presented.

A deep discussion about the results and their application to sensing proteins and triblock copolymers is presented.

2. MATERIALS AND METHODS

2.1. Materials and Solutions. Pluronic P103 (average molecular weight, 4950 g mol^{-1}) was obtained from BASF, and BSA protein (average molecular weight, 66,430 g mol^{-1}) was acquired from Sigma-Aldrich. Both reagents were used as received. A 0.1 M phosphate buffer solution (PBS), containing 8 g L^{-1} NaCl, 0.2 g L^{-1} KCl, 2.68 g L^{-1} $Na_2HPO_4{\cdot}5H_2O$, and 0.216 g L^{-1} NaH_2PO_4 was used to maintain each studied solution at a pH of 7.2−7.4. The above PBS solution was used to prepare three different solutions: (i) pure P103 (0.6 wt %, corresponding to 6 g L^{-1}), (ii) pure BSA (3 mg mL^{-1}), and (iii) mixtures of P103-BSA (0.6 wt % and 3 mg mL^{-1}, respectively). The selected BSA concentration was in the range typically studied in other works,[18] while the P103 concentration was selected to ensure a micellar structure.[20]

A scheme of the solution preparation is shown in Figure 1. All solutions were prepared with HPLC grade water.

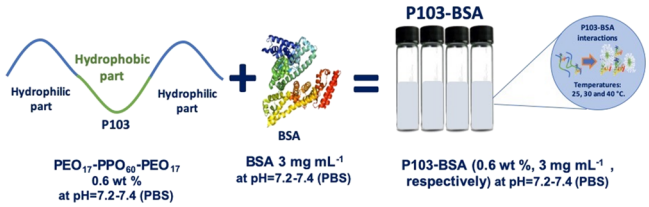

Figure 1. Solution preparation: schematic representation.

2.2. Electrochemical Measurements. A typical three-electrode cell was used. The working electrode was a gold disc electrode (2 mm in diameter, 0.031 cm^2), a platinum electrode was used as the counter electrode, and a saturated calomel electrode (SCE) was used as the reference electrode. Before any experiment, the working electrode was first polished with an alumina slurry of 0.5 μm, rinsed with distilled water, and dried with compressed air.

The electrochemical response of P103 and BSA pure solutions and P103-BSA solutions in PBS medium was acquired first by CV and then by EIS at the concentrations cited above. The experiments were performed at 25, 30, and 40 °C.

The CV measurements were obtained in the potential range of −1 to 1 V vs SCE at 100 mV/s in 0.1 M PBS. Two different kinds of EIS experiments were carried out. The first experiments were performed at the open-circuit potential (OCP). A potential perturbation amplitude of 10 mV and a frequency range of 10 kHz to 1 mHz were applied. Seven points per logarithmic decade were taken.

The double-layer capacitance response as a function of the polarization potential was obtained from another set of EIS experiments performed at 100 Hz and 10 mV of amplitude (these kinds of experiments are also known as AC voltammetry).

https://dx.doi.org/10.1021/acsomega.0c01704
ACS Omega 2020, 5, 17347−17355

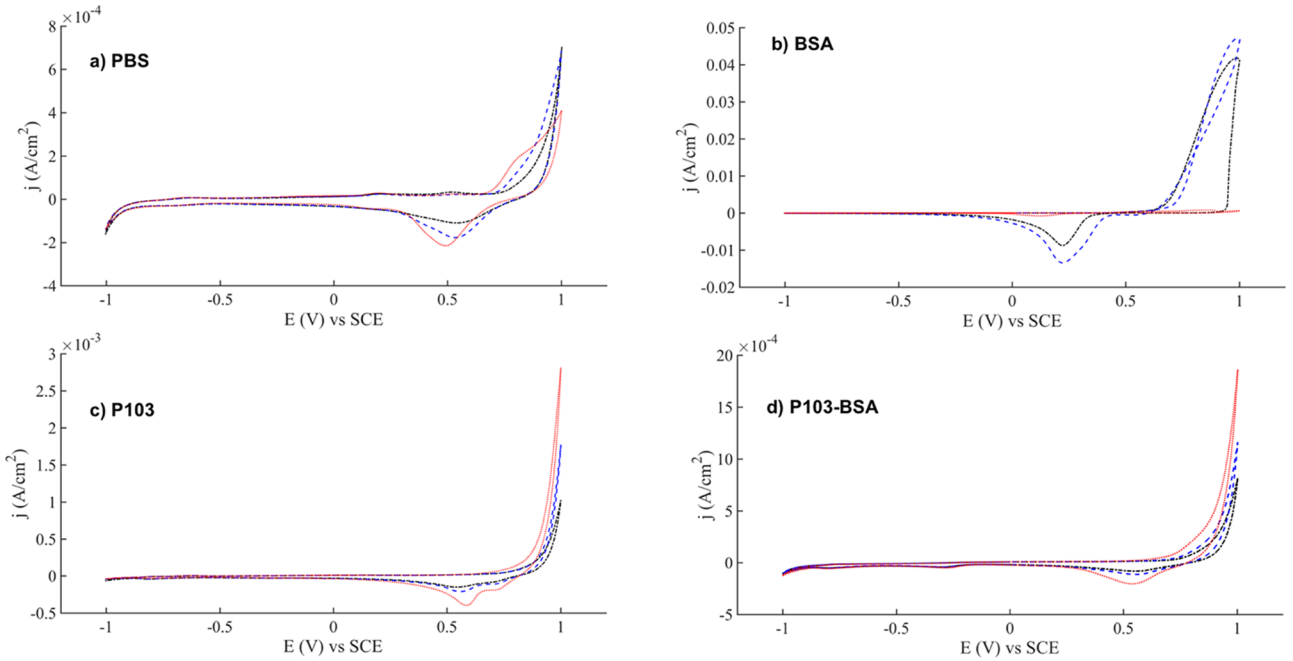

Figure 2. Typical voltammetric responses for (a) Au/PBS, (b) Au/BSA, (c) Au/P103, and (d) Au/P103-BSA (P103 0.6 wt %, BSA 3 mg mL^{-1}). Black, blue, and red lines for 25, 30, and 40 °C, respectively.

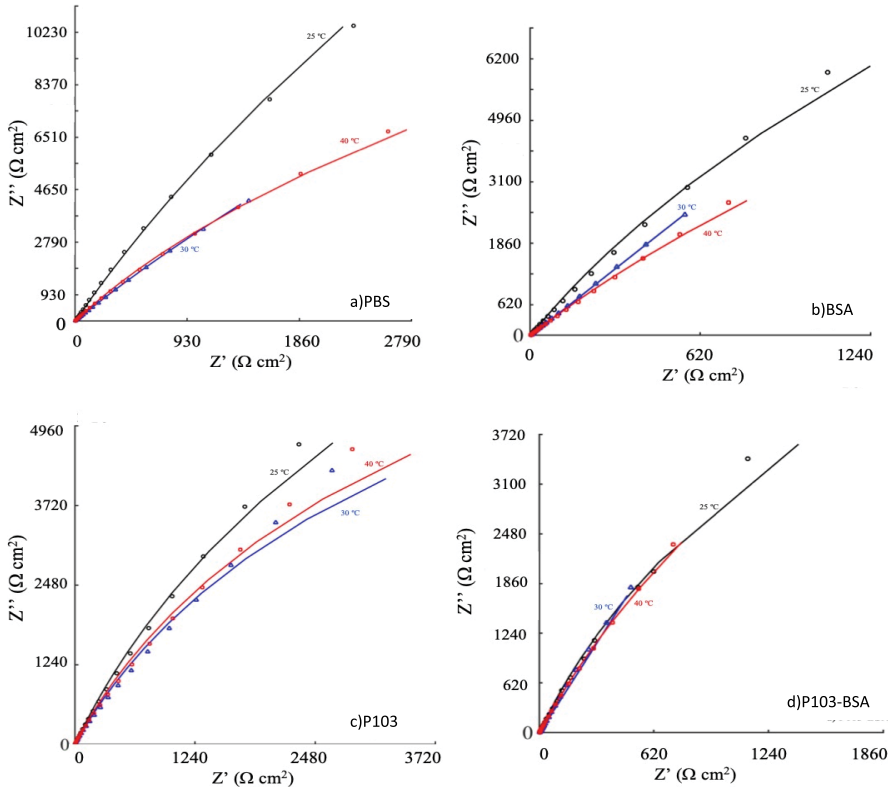

Figure 3. Nyquist diagrams obtained at the OCP for (a) Au/PBS, (b) Au/BSA, (c) Au/ P103, and (d) Au/P103-BSA (P103 0.6 wt %, BSA 3 mg mL^{-1}). Black, blue, and red lines for 25, 30, and 40 °C, respectively.

The same polarization range used in the CV was used for the EIS measurements, but a sweep of 1 mV/s was employed to ensure the quasi-steady state of the system. The double-layer capacitance vs polarization potential curves were computed from the imaginary part of these impedance measurements.

All measurements were carried out using an Autolab potentiostat (PGSTAT 128N).

3. RESULTS AND DISCUSSION

3.1. Voltammetry Characterization Experiments. First, the electrochemical response was examined through the

https://dx.doi.org/10.1021/acsomega.0c01704
ACS Omega 2020, 5, 17347−17355

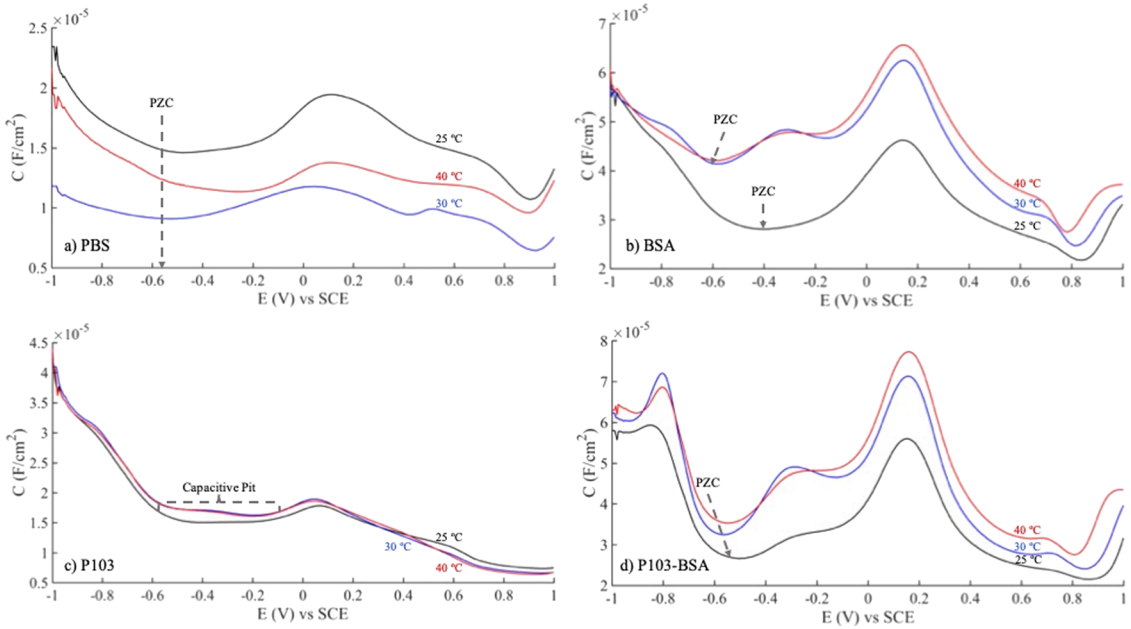

Figure 4. Double-layer capacitance curves for (a) Au/PBS, (b) Au/BSA, (c) Au/ P103, and (d) Au/P103-BSA (P103 0.6 wt %, BSA 3 mg mL^{-1}). Black, blue, and red lines for 25, 30, and 40 °C, respectively.

voltammetric profiles of the gold electrode immersed in pure 0.1 M PBS, BSA, and P103 pure solutions; subsequently, the electrochemical response of the mixture of P103-BSA in PBS medium was analyzed. The typical voltammetric responses of each of the studied solutions are shown in Figure 2.

Since the interaction of P103 and BSA molecules and their adsorption onto gold electrodes in natural conditions imply the absence of any faradaic process, the analysis of the voltammetric responses is centered in the polarization potential interval where the interface behaves as ideally polarizable. As seen in Figure 2a, the voltammetric response for a pure PBS solution shows that, in a polarization potential range from −0.6 to 0.1 V vs SCE, the faradaic process is absent at the interface.

In a polarization potential range from 0.1 to 0.4 V vs SCE, the faradaic current observed in Figure 2a can be associated with a slight oxidation−reduction of phosphate ions, while from 0.4 to 1 V vs SCE, the faradaic current response is associated with the electrochemical response of the gold electrode.[31] On the other hand, as observed in Figure 2b−d, the interface remains similar to that observed in Figure 2a. However, some appreciable changes in the current magnitude are detected. Figure 2b reveals that BSA at 3 mg mL^{-1} strongly enhances the oxidation, dissolution, and reduction processes of the gold substrate and thus modifies the polarization potential range at which that process occurs. This behavior is more evident at 25 and 30 °C. Conversely, when 0.6 wt % P103 is present in Figure 2c, the current associated with the electrochemical process of the gold substrate decreases, and a small cathodic peak, associated with some P103 reduction, is observed at approximately 0.75 V vs SCE. This reduction peak can be associated with the reduction of PEO, as has been previously evidenced.[30] Furthermore, the presence of P103 inhibits the oxidation−reduction process of phosphate ions observed in Figure 2a. Nevertheless, when BSA interacts with P103, as shown in Figure 2d, the polarization range where the interface does not present any charge transfer increases, revealing that the mixture of P103-BSA remains stable in the polarization interval from −0.75 to 0.2 V vs SCE.

3.2. EIS and Electrochemical Double-Layer Capacitance Curves. Figure 3 shows the response obtained from the first set of EIS experiments. As observed at all temperatures, the typical Nyquist diagrams depict the beginning of a large capacitive loop for the three systems studied. This behavior is consistent with the OCP experimental condition corresponding to null current flowing through the interface.

The impedance responses show a non-ideal double-layer capacitance behavior associated with the electrochemical double-layer rearrangements, which are clearly sensitive to the presence of BSA and P103 in a pure solution and the interaction of P103-BSA molecules, as depicted by the frequency impedance distribution observed in Figure 3b−d.

More detailed information concerning the interaction between the adsorbate and substrate and its associated response to the electrochemical double layer is acquired through the double-layer capacitance curves calculated using the second set of EIS measurements. In these curves, the effect of the polarization potential on the double-layer capacitance is shown, and the polarization range where the adsorption and interaction between the substrate and adsorbate are enhanced or inhibited is determined. Figure 4a−d shows the double-layer capacitance C for pure 0.1 M PBS, BSA at 3 mg mL^{-1}, 0.6 wt % P103, and P103-BSA solution at the cited concentrations in PBS medium, respectively. The effect of a wide polarization range at the three studied temperatures is demonstrated.

An analysis of the double-layer capacitance curves allowed the potential of zero charge (PZC) for each one of the interfaces to be obtained. Based on the classical capacitance double-layer theory, the PZC is located between two maxima.[32,33] For a capacitive process, the double-layer capacitance reaches its minimum in a polarization potential range where faradaic reactions are negligible. This polarization range was previously determined by CV. It should be noted that, when Figure 4 shows at least two local minima for each system, the one observed at positive potentials is related to the changes of the interface due to the faradaic process associated with either the PBS, BSA, or P103 compounds or oxidation of the gold substrate. The above

https://dx.doi.org/10.1021/acsomega.0c01704
ACS Omega 2020, 5, 17347−17355

Table 1. Summary of the Double-Layer and Adsorption Properties for Au/PBS, Au/BSA, and Au/P103 Interfaces (P103 0.6 wt %, BSA 3 mg mL^{-1})

interface	adsorbate, charge	PZC	favorable adsorption	observations
Au/PBS	phosphates, negative	−0.55 V	0.15 V > *E* > −0.55 V at all temperatures	adsorption of phosphates
Au/BSA (in PBS medium)	protein, positive	25 °C −0.4 V	−0.4 V > *E* > −1 V	phosphates and protein adsorption from −0.4 to −0.55 V
		30 °C −0.6 V	−0.6 V > *E* > −1 V	protein adsorption
		40 °C −0.6 V	−0.6 V > *E* > −1 V	protein adsorption
Au/P103 (in PBS medium)	P103, neutral		0.1 V > *E* > −0.6 V at all temperatures	capacitive pit, adsorption of P103 and phosphates

results can also be observed in Figure 2a−d. Thus, the PZC for each of the interfaces studied is located at negative polarization potentials, and the following discussion concerns this polarization zone.

The Au/PBS interface (Figure 4a) presents its PZC at approximately −0.55 V vs SCE. The PZC is clearly observed by a broad minimum that slightly varies as a function of temperature. The temperature effect is more clearly evidenced in the interfacial double-layer capacitance values, where the lowest values are reached at 30 °C (blue line), while the highest values are obtained at 25 ° C (black line). In agreement with Figure 4a and according to the double-layer capacitance theory,[32,33] for polarization potentials more positive than PZC, −0.55 V vs SCE, the working electrode possesses a positive charge, and subsequently, the phosphate ions are adsorbed onto its surface until the polarization potential reaches 0.15 V vs SCE. At this polarization potential, a maximum in the double-layer capacitance curve defines the end of the capacitive response, and the beginning of faradaic effects on the double-layer capacitance behavior begins.

According to Figure 4b, the interface changes its capacitive behavior in the presence of BSA solution in PBS medium. The double-layer capacitance curves show that the PZC strongly depends on both the temperature and polarization potential. In this way, a very well-defined minimum at approximately −0.6 V vs SCE. is obtained at 30 and 40 °C (blue and red lines, respectively), while at 25 °C (black line), a wide polarization zone achieves lower values for the double-layer capacitance, reaching its minimum value at approximately −0.4 V vs SCE. It should be noted that, regardless of the temperature effect, in all cases, the electrode has a negative charge at more negative potentials than each of the PZCs found in Figure 4b. The adsorption of BSA on the gold electrode will depend on both the substrate and the BSA charge. The charge of the BSA molecule is influenced by the pH of the medium. Since BSA possesses an isoelectric point at a pH of 4.7,[34] it will present a positive charge at the pH used in this work. Then, the adsorption of BSA is favorable at more negative polarization potentials than the observed PZC for the Au/BSA interface. Taking this into account and according to the PZC obtained in Figure 4a,b at 25 °C, a competitive adsorption of phosphate ions and the BSA protein is presented in a polarization range from −0.4 to −0.55 V vs SCE, while at more negative potentials, only the protein adsorption is greater. Competitive adsorption is not present at the highest temperatures (30 and 40 °C), where only the adsorption of the protein is favorable at more negative polarization potentials than the PZC.

On the other hand, in Figure 4b, at 30 and 40 °C, in addition to the polarization zone in which the interface gets its PZC, the capacitance curves depict a shoulder at −0.3 V vs SCE. This behavior has also been observed in other interfaces,[33,35] and as observed in those interfaces, the shoulder is related to a relaxation and rearrangement of the interface, which in turn could imply the desorption of the protein caused by the positive charge at the electrode and the adsorption process of the phosphate ions. These processes change the behavior of the interface and modify the double-layer capacitance response, causing the feature response observed in the curve.

The changes in the double-layer capacitance response as a function of the temperature are almost negligible when a pure P103 solution in PBS medium is studied, as shown in Figure 4c. As observed, the double-layer capacitance does not show any minima but instead exhibits a polarization zone from −0.6 to 0.1 V vs SCE, where the capacitance curves present the typical "pit" associated with the adsorption of neutral molecules such as triblock copolymers.[33,36,37] In this polarization range, the adsorption of P103 is favorable. Furthermore, since the P103 is in PBS medium, it should be highlighted that, according to Figure 4a, phosphate ions should also be adsorbed in a polarization range from −0.55 to 0.15 V vs SCE. However, according to Figure 4c, P103 adsorption prevails.

Table 1 summarizes the behavior of the studied interfaces and presents the polarization range in which adsorptions are favorable.

On the other hand, Figure 4d presents the modification of the double-layer capacitance when the gold electrode is immersed in the P103-BSA in PBS medium. In this case, the behavior of the capacitance curves depicts a similar behavior to that observed for a solution of PBS containing only the protein (Figure 4b); however, more pronounced changes in the double-layer capacitance values are observed in a polarization potential range between −0.8 and 0.18 V vs SCE. Furthermore, the minimum associated with the PZC is slightly different from that observed in Figure 4b, reaching a polarization potential ranging from −0.56 to −0.5 V vs SCE, depending on the temperature. The similarity in the capacitance curve profiles observed in Figure 4b,d is more evident at the highest temperatures (blue and red lines), while at 25 °C (black line), the shape of the capacitance curve reaches lower values in a narrower polarization zone (−0.5 V vs SCE) compared to the response obtained in the absence of P103. It should be noted that, in all the temperatures tested, Figure 4d shows a more pronounced shoulder compared to the one observed in Figure 4b. This pronounced shoulder is associated with a more prominent relaxation and rearrangement of the interface caused by the interactions between PBS, BSA, P103, and the electrode. According to Table 1 and the PZC obtained in Figure 3d, the interface relaxation and its rearrangements include the competitive adsorption of phosphate ions and P103 copolymer, along with BSA desorption.

The behavior of double-layer capacitance, observed in Figure 4, is sensitive enough to detect the changes in the interphase

https://dx.doi.org/10.1021/acsomega.0c01704
ACS Omega 2020, 5, 17347−17355

induced by the presence of each species studied in an isolated manner and their interactions when all of them are added to the working solution.

The charge of the electrode and the preferential adsorption of certain adsorbates strongly depend on the polarization potential. Envisaging the utility of this study in the fields of biomedicine and bioengineering for the design of sensors, an analysis of the Au/P103-BSA interface at the open-circuit potential (OCP) is quite interesting. For the conditions presented in Figure 4d, the OCP is approximately 0.14 V vs SCE. At this polarization potential, the electrode possesses a positive charge, and the desorption of BSA occurs. At the same time, the phosphates and neutral P103 polymer are at the polarization potential limit where their adsorption is electrostatically favorable but are tending to begin their desorption. If the interaction and adsorption of P103 and BSA is required, then a polarization potential more negative than OCP, which avoids the electrochemical denaturation of the protein, should be fixed for the electrode. For instance, at −0.6 V vs SCE, the adsorption of P103 and BSA as well as interactions among them is highly plausible. Additionally, according to Figure 2, at this polarization potential, no electrochemical reaction is affecting the protein. Thus, it is proven that well-defined changes in the double-layer capacitance values, as shown in Figure 4d, allow sensing the adsorption/desorption process and qualitatively reveals interactions between the protein and the triblock copolymer.

3.3. Apparent Interface Thickness. Even though the polarization potential and temperature are parameters that strongly modify the values of the double-layer capacitance as well as the substrate charge, other properties influence the double-layer structure, such as those inherent to the adsorbates, i.e., charge, structure, and conformation. These last properties are closely related to the interface thickness and its dielectric nature.

The simplest model of the electrochemical double-layer theory[33] establishes that the double-layer capacitance value C is inversely proportional to the interface thickness d, according to the following equation:

$$C = \frac{\varepsilon\varepsilon_0}{d} \tag{1}$$

where ε_0 and ε are the permittivities of vacuum and the medium, respectively.

If the permittivity of the medium is known and the double-layer capacitance values are measured, as in this study, the interface thickness can be calculated. However, the permittivity value of the PBS/P103-BSA mixed medium has not been previously reported. The permittivities of some triblock copolymers and BSA have been studied independently, and the main results are known.[37−40] It is well known that the dielectric constant of P103 strongly depends on its mass fraction %, reaching an average value of approximately 1.5 for P103 between zero and 50 wt %.[39] On the other hand, numerous values of the dielectric constant for BSA are reported without consensus.[41] It is accepted that the dielectric constant value of BSA depends on the frequency, hydration, temperature, and weight percentage. Dielectric values ranging from 4 to 70 are reported.[34] In general, the frequency dielectric dispersion of BSA is reported and related to its own protein relaxations, which are associated to its structure and sequence.[40,41]

Thus, even when the interface thickness d cannot be calculated from eq 1, the permittivity value for the mixed medium, PBS/P103-BSA, is required; the relation of ε_0/C, which is known, can be calculated from eq 1 to obtain the apparent interface thickness parameter d^*, as shown in eq 2:

$$d^* = \frac{\varepsilon_0}{C} = \frac{d}{\varepsilon} \tag{2}$$

where d^* is the relation of the double-layer length and the variation of the medium permittivity. The value of d^* can bring some qualitative and indirect insight into the structure or conformation in which P103 and BSA interact and become adsorbed at the gold electrode. Similar approximations have been performed previously in other studies.[42−44]

Figure 5 shows the variations of the apparent interface thickness d^* as a function of the polarization potential where

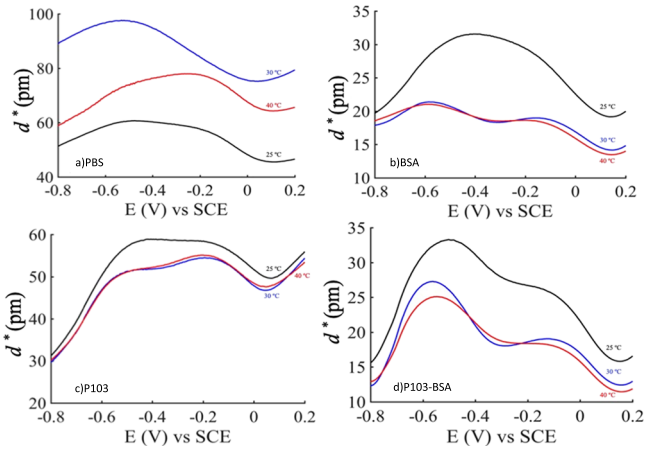

Figure 5. Apparent interface thickness as a function of polarization potentials for (a) Au/PBS, (b) Au/BSA, (c) Au/P103, and (d) Au/P103-BSA (P103 0.6 wt %, BSA 3 mg mL^{-1}). The apparent interface thicknesses were calculated from eq 2. Black, blue, and red lines for 25, 30, and 40 °C, respectively.

faradaic reactions are absent. The effect of the three studied temperatures is presented. The apparent interface thickness is calculated by capacitance data shown in Figure 4, the value of the permittivity of vacuum, and eq 2.

As observed in Figure 5, we can conclude that, at all the temperatures and for the whole polarization range, the apparent interface thickness reaches its greatest values when the gold electrode is immersed in pure PBS solution (Figure 5a) and suggests that the double-layer structure is not compact but diffuse.

The above finding is in good agreement with the well-known weak adsorption of phosphate ions, which are related to the ion size and solvation energies and are translated into a broad electrochemical double-layer structure, as concluded by Anson.[45] However, the structure of the electrochemical double layer, associated with d^*, is clearly modified when BSA and P103 are present. For instance, at approximately −0.6 V vs SCE, when adsorption of both BSA and P103 is favorable, the interface becomes more compact, reaching intermediate apparent thickness values for P103 (Figure 5c). The thickness decreases in a more accentuated way when BSA and P103 are interacting (Figure 5d), and the electrochemical double layer reaches the most compact apparent thickness in the presence of BSA (Figure 5b). The apparent thickness shown in Figure 5d at −0.6 V vs SCE could be presumably associated with the protein−P103 interaction as a global species; however, the acquisition of a particular conformation requires other studies.

https://dx.doi.org/10.1021/acsomega.0c01704
ACS Omega 2020, 5, 17347−17355

The apparent thickness values and behavior obtained in Figure 5b,d are similar. This behavior is also observed in the double-layer capacitance curves. The apparent thickness of the interface presents an appreciable change in its shape at a polarization of approximately −0.3 V vs SCE. This effect confirms the relaxation of the interface, which in turn can be associated with a change in the structure or conformation of the adsorbate.[33,35]

On the other hand, in Figure 5b−d, it is evident that increasing the temperature induces a decrease in the apparent thickness of the electrochemical double layer. Thus, the adsorption of proteins could be similarly seen as the adsorption of organic molecules on metal electrodes, where it causes a decrease in the double-layer capacitance values.[12,42]

If the analysis is performed around 0.14 V vs SCE, corresponding to the OCP, it is possible to note from Figure 5d that the interface has lower apparent thickness values, reaching 17, 13, and 11 pm for 25 (black line), 30 (blue line), and 40 °C (red line), respectively. These values are appreciably lower than those obtained at 0.14 V vs SCE for Au/PBS (Figure 5a), Au/PBS+BSA (Figure 5b), and Au/PBS+P103 (Figure 5c). Considering that, at this polarization potential, the BSA protein is not being adsorbed, the results indicate that at 0.14 V vs SCE; the presence of either phosphate ions or P103 copolymer inside the interphase and their adsorption on the electrode is incipient, so the apparent thickness is low. This fact emphasizes that, at the OCP, the P103 and phosphate ions tend to be desorbed, which is in good agreement with the discussion presented in the previous section. Thus, d^* is sensitive to the adsorption−desorption and interaction of the studied adsorbates.

If the highest interaction between the phosphate ions and both the protein and the Pluronic is required, a more negative polarization potential than the OCP shall be applied to the substrate, as is stated in the previous section. According to the double-layer capacitance curves and Table 1, a polarization potential between −0.5 and −0.6 V vs SCE is adequate to induce the interaction of P103 and BSA and its adsorption as a global species. As can be noted in Figure 5d, in a polarization potential range from −0.5 to −0.6 V vs SCE, the interface acquires greater apparent thickness values of approximately 33, 27, and 24 pm at 25 (black line), 30 (blue line), and 40 °C (red line), respectively. These apparent thickness values are higher than those obtained at the OCP, which can be related to the adsorption of BSA and P103 polymer. Furthermore, according to the well-differentiated curve shape and the values obtained, the double-layer capacitance measurements and the calculation of the apparent interface thickness through eq 2 is considered an adequate analytical method for sensing the protein−triblock polymer interactions.

It should be noted that, even when at −0.5 to −0.6 V vs SCE, the adsorption of phosphate ions is not favorable, the phosphate ion presence will influence the ionic strength, and then the interaction between BSA and P103 will clearly modify the structure of the BSA protein. It is well known that several structures are possible for the adsorption of pluronics[46−50] and proteins.[5,51,52] These structures are dependent on the ionic strength of the medium,[53] which in our study is given by the phosphate ions.

Subsequently, it should be noted that the conformation and structure of the adsorbed global species strongly depends either on the critical micellar concentration (cmc) or temperature (cmt) of the P103 triblock polymer as well as the structural conformation of the protein. For the particular case of the H_2O/P103 triblock polymer, accurate phase diagrams are already published,[46,47] and as a consequence, the microstructure formed by P103 is well known. However, these structures cannot be considered in this work because the buffer used has a different ionic strength that modifies the P103 physical properties, mainly its conformational structure. Furthermore, the adsorption of surfactants on surfaces could lead to the formation of adsorbed structures as admicelles or hemimicelles. The same consideration is valid for the conformations of BSA.[51−53] Due to its nature as a natural polyelectrolyte, its structure strongly depends on the ionic strength of the buffer. Consequently, a new phase diagram using further techniques, such as rheological, optical, or dispersion, is required to obtain the microstructure and conformation of the global species adsorbed on the electrode.

3.4. Significance, Impact, and Possible Future Work.

The development of biosensors, biomaterials, biochips, and modified nanoparticles for drug delivery, along with other technologically applied fields, requires a deep understanding of the biomolecule-modified substrate interactions and the implementation of an optimal analytical method to detect them in an accurate way.

Concerning the albumin proteins and triblock copolymer interactions, this work successfully demonstrates that using simple electrochemical techniques is viable. The electrostatic effect plays an important role in the mechanism of interaction and influences the adsorption between BSA and P103 copolymer, showing that at −0.6 V vs SCE, a strong interaction is reached. Obtaining optimal polarization ranges where the interaction is maximum is a key topic for biomaterials and self-organized film template development, as demonstrated in the studies presented by Palacio et al.,[54] Liu et al.,[55] Chang et al.,[56] and others.[57] Furthermore, by using electrochemical methods, the use of more sophisticated techniques, such as those used in,[54,55] namely, atomic force microscopy, small-angle X-ray, and other physical methods, is avoided.

On the other hand, the detection of albumin proteins is important due to its essential function in blood plasma. Colorimetry and fluorescence spectroscopy are techniques used for their detection; however, both have disadvantages in their estimation or selectivity.[23] Some selective albumin sensors have been designed; however, they have shown inconveniencies related to their complex fabrication, control, or cost. The molecularly imprinted electrochemical sensors using macromolecular templates[23,24] or those in which more sophisticated electrodes such as semiconductors[14] or coated-quartz crystal resonators[16,54] are used are representative examples of this type of sensor. According to our results, a conventional gold electrode immersed in P103 triblock copolymer solution is sensitive to the interactions and adsorption/desorption process of BSA, which is evidenced by well-defined changes in double-layer capacitance values or the behavior of the apparent interface thickness as a function of polarization potentials. In this way, the experimental setup and the double-layer capacitance measurements presented in this work are considered a possible analytical method to sense, in a simple way, the interactions between BSA and P103. However, validation of this method requires further research.

4. CONCLUSIONS

A fundamental and analytical electrochemical adsorption study of PBS, BSA protein, and P103 triblock copolymer onto a gold electrode was conducted via EIS measurements and double-layer capacitance curves using a wide polarization range at three different temperatures. A detailed analysis of these curves

https://dx.doi.org/10.1021/acsomega.0c01704
ACS Omega 2020, 5, 17347−17355

allowed us to detect the interactions between PBS-BSA-P103 molecules.

From the obtained double-layer capacitance curves, it was possible to determine the PZC for each of the interfaces studied. A discussion concerning the polarization potential range in which the adsorption of each species studied is favorable is presented in detail. Furthermore, based on the simplest model of the electrochemical double-layer theory, the apparent interface thickness was obtained.

The results help provide understanding of the electrostatic effect during the interaction of PBS, BSA, and P103 in the interface. The focus was on the OCP, where the lowest double-layer apparent thickness values are obtained, showing that, at this polarization potential, the adsorption of BSA is electrostatically impeded while the desorption of phosphate ions and P103 copolymer begins.

The interaction of P103 and BSA and its adsorption is only favorable at more negative polarization potentials than the OCP. The optimal polarization potential is between −0.5 and −0.6 V vs SCE, where BSA and P103 are adsorbed as a global species, causing a higher apparent interface thickness of approximately 33, 27, and 24 pm at 25, 30, and 40 °C, respectively.

The acquisition of a particular conformation and structure of adsorbate PBS-BSA and P103, as a global species, requires further studies using other techniques, such as rheological, optical, or dispersive methods.

AUTHOR INFORMATION

Corresponding Author

Erika Roxana Larios-Durán − *Departamento de Ingeniería Química, Universidad de Guadalajara, 44430 Guadalajara, Jalisco, México;* orcid.org/0000-0002-0945-3546; Phone: +52 33 13785900; Email: roxlarios@icloud.com

Authors

Brenda Velasco-Rodriguez − *Departamento de Ingeniería Química, Universidad de Guadalajara, 44430 Guadalajara, Jalisco, México*

J. Félix Soltero-Martínez − *Departamento de Ingeniería Química, Universidad de Guadalajara, 44430 Guadalajara, Jalisco, México*

Luis Carlos Rosales-Rivera − *Departamento de Ingeniería Química, Universidad de Guadalajara, 44430 Guadalajara, Jalisco, México*

Emma Rebeca Macías-Balleza − *Departamento de Ingeniería Química, Universidad de Guadalajara, 44430 Guadalajara, Jalisco, México*

Gabriel Landázuri − *Departamento de Ingeniería Química, Universidad de Guadalajara, 44430 Guadalajara, Jalisco, México*

Complete contact information is available at: https://pubs.acs.org/10.1021/acsomega.0c01704

Notes

The authors declare no competing financial interest.

ACKNOWLEDGMENTS

B.V.-R. is grateful to CONACyT for financial support for his Ph.D. studies. The authors also wish to thank CONACyT for project grant number 223549.

REFERENCES

(1) Hamza, S.; Bouchemi, M.; Slimane, N.; Azari, Z. Physical and Chemical Characterization of Adsorbed Protein onto Gold Electrode Functionalized with Tunisian Coral and Nacre. *Mater. Sci. Eng. C* **2013**, *33*, 537−542.

(2) Hepel, M.; Stobiecka, M. Interactions of Adsorbed Albumin with Underpotentially Deposited Copper on Gold Piezoelectrodes. *Bioelectrochemistry* **2007**, *70*, 155−164.

(3) Wang, J.; Rivas, G.; Jiang, M.; Zhang, X. Electrochemically Induced Release of DNA from Gold Ultramicroelectrodes. *Langmuir* **1999**, *15*, 6541−6545.

(4) Haruyama, T.; Sakai, T.; Matsuno, K. Protein Layer Coating Method on Metal Surface by Electrochemical Process through Genetical Introduced Tag. *Biomaterials* **2005**, *26*, 4944−4947.

(5) Tengvall, P.; Askendal, A.; Lundström, I. Studies on Protein Adsorption and Activation of Complement on Hydrated Aluminium Surfaces in Vitro. *Biomaterials* **1998**, *19*, 935−940.

(6) Villar-Alvarez, E.; Figueroa-Ochoa, E.; Barbosa, S.; Soltero, J. F. A.; Taboada, P.; Mosquera, V. Reverse Poly(Butylene Oxide)-Poly-(Ethylene Oxide)-Poly(Butylene Oxide) Block Copolymers with Lengthy Hydrophilic Blocks as Efficient Single and Dual Drug-Loaded Nanocarriers with Synergistic Toxic Effects on Cancer Cells. *RSC Adv.* **2015**, *5*, 52105−52120.

(7) Figueroa-Ochoa, E. B.; Villar-Alvarez, E. M.; Cambón, A.; Mistry, D.; Llovo, J.; Attwood, D.; Barbosa, S.; Soltero, J. F. A.; Taboada, P. Lenghty Reverse Poly(Butylene Oxide)-Poly(Ethylene Oxide)-Poly-(Butylene Oxide) Polymeric Micelles and Gels for Sustained Release of Antifungal Drugs. *Int. J. Pharm.* **2016**, *510*, 17−29.

(8) Yang, X.; Too, C. O.; Sparrow, L.; Ramshaw, J.; Wallace, G. G. Polypyrrole-Heparin System for the Separation of Thrombin. *React. Funct. Polym.* **2002**, *53*, 53−62.

(9) Jackson, D. R.; Omanovic, S.; Roscoe, S. G. Electrochemical Studies of the Adsorption Behavior of Serum Proteins on Titanium. *Langmuir* **2000**, *16*, 5449−5457.

(10) Trzeciakiewicz, H.; Esteves-Villanueva, J.; Soudy, R.; Kaur, K.; Martic-Milne, S. Electrochemical Characterization of Protein Adsorption onto YNGRT-Au and VLGXE-Au Surfaces. *Sensors* **2015**, *15*, 19429−19442.

(11) Heli, H.; Sattarahmady, N.; Jabbari, A.; Moosavi-Movahedi, A. A.; Hakimelahi, G. H.; Tsai, F.-Y. Adsorption of Human Serum Albumin onto Glassy Carbon Surface - Applied to Albumin-Modified Electrode: Mode of Protein-Ligand Interactions. *J. Electroanal. Chem.* **2007**, *610*, 67−74.

(12) Moulton, S. E.; Barisci, J. N.; Bath, A.; Stella, R.; Wallace, G. G. Studies of Double Layer Capacitance and Electron Transfer at a Gold Electrode Exposed to Protein Solutions. *Electrochim. Acta* **2004**, *49*, 4223−4230.

(13) Sotiropoulos, S.; Avranas, A.; Papadopoulos, N. Study of Oleate Adsorption at the Mercury/Electrolyte Solution Interface as a Function of Electrode Potential and Time. *Langmuir* **1997**, *13*, 7230−7238.

(14) Oliva, F. Y.; Cámara, O. R.; Avalle, L. B. Adsorption of Human Serum Albumin on Electrochemical Titanium Dioxide Electrodes: Protein-Oxide Surface Interaction Effects Studied by Electrochemical Techniques. *J. Electroanal. Chem.* **2009**, *633*, 19−34.

(15) Omanovic, S.; Roscoe, S. G. Electrochemical Studies of the Adsorption Behavior of Bovine Serum Albumin on Stainless Steel. *Langmuir* **1999**, *15*, 8315−8321.

(16) Lori, J. A.; Hanawa, T. Adsorption Characteristics of Albumin on Gold and Titanium Metals in Hanks' Solution Using EQCM. *Spectroscopy* **2004**, *18*, 545−552.

(17) Alatorre-Meda, M.; Taboada, P.; Sabín, J.; Krajewska, B.; Varela, L. M.; Rodríguez, J. R. DNA-Chitosan Complexation: A Dynamic Light Scattering Study. *Colloids Surf., A* **2009**, *339*, 145−152.

(18) Yasseen, Z. G. On the Interactions of Bovine Serum Albumin with Some Surfactants: New Insights from Conductivity Studies. *J. Chem. Pharm. Res.* **2012**, *4*, 3361−3367.

(19) Mishra, S.; Peddada, L. Y.; Devore, D. I.; Roth, C. M. Poly(Alkylene Oxide) Copolymers for Nucleic Acid Delivery. *Acc. Chem. Res.* **2012**, *45*, 1057−1066.

(20) Neacsu, M. V.; Matei, I.; Micutz, M.; Staicu, T.; Precupas, A.; Popa, V. T.; Salifoglou, A.; Ionita, G. Interaction between Albumin and Pluronic F127 Block Copolymer Revealed by Global and Local Physicochemical Profiling. *J. Phys. Chem. B* **2016**, *120*, 4258−4267.
(21) Green, R. J.; Davies, J.; Davies, M. C.; Roberts, C. J.; Tendler, S. J. B. Surface Plasmon Resonance for Real Time in Situ Analysis of Protein Adsorption to Polymer Surfaces. *Biomaterials* **1997**, *18*, 405−413.
(22) Brandani, P.; Stroeve, P. Adsorption and Desorption of PEO-PPO-PEO Triblock Copolymers on a Self-Assembled Hydrophobic Surface. *Macromolecules* **2003**, *36*, 9492−9501.
(23) Cieplak, M.; Szwabinska, K.; Sosnowska, M.; Chandra, B. K. C.; Borowicz, P.; Noworyta, K.; D'Souza, F.; Kutner, W. Selective Electrochemical Sensing of Human Serum Albumin by Semi-Covalent Molecular Imprinting. *Biosens. Bioelectron.* **2015**, *74*, 960−966.
(24) Xia, J.; Cao, X.; Wang, Z.; Yang, M.; Zhang, F.; Lu, B.; Li, F.; Xia, L.; Li, Y.; Xia, Y. Molecularly Imprinted Electrochemical Biosensor Based on Chitosan/Ionic Liquid-Graphene Composites Modified Electrode for Determination of Bovine Serum Albumin. *Sens. Actuators, B* **2016**, *225*, 305−311.
(25) Liou, Y.-B.; Tsay, R.-Y. Adsorption of PEO-PPO-PEO Triblock Copolymers on a Gold Surface. *J. Taiwan Inst. Chem. Eng.* **2011**, *42*, 533−540.
(26) Rana, D.; Bag, K.; Bhattacharyya, S. N.; Mandal, B. M. Miscibility of Poly(styrene-co-butyl acrylate) with Poly(ethyl methacrylate): Existence of Both UCST and LCST. *J. Polym. Sci., Part B: Polym. Phys.* **2000**, *38*, 369−375.
(27) Rana, D.; Mandal, B. M.; Bhattacharyya, S. N. Miscibility and phase diagrams of poly(phenyl acrylate) and poly(styrene-co-acrylonitrile) blends. *Polymer* **1993**, *34*, 1454−1459.
(28) Rana, D.; Mandal, B. M.; Bhattacharyya, S. N. Analogue calorimetry of polymer blends: poly(styrene-co-acrylonitrile) and poly(phenyl acrylate) or poly(vinyl benzoate). *Polymer* **1996**, *37*, 2439−2443.
(29) Rana, D.; Mandal, B. M.; Bhattacharyya, S. N. Analogue calorimetric studies of blends of poly(vinyl ester)s and polyacrylates. *Macromolecules* **1996**, *29*, 1579−1583.
(30) Ohno, H.; Tsukuda, T. Electron-transfer reaction of polyethylene oxide-modified myoglobin in polyethylene oxide oligomers. *J. Electroanal. Chem.* **1992**, *341*, 137−149.
(31) Luk, V. N.; Mo, G. C.; Wheeler, A. R. Pluronic Additives: A Solution to Sticky Problems in Digital Microfluidics. *Langmuir* **2008**, *24*, 6382−6389.
(32) Ramírez-Rico, D. S.; Larios-Durán, E. R. Electrochemical Study on Electrodissolution of Gold in Acidic Medium Using Chlorides as Ligands. *J. Electrochem. Soc.* **2017**, *164*, H994−H1002.
(33) Devanathan, M. A. V.; Tilak, B. V. K. S. R. A. The Structure of the Electrical Double Layer at the Metal-Solution Interface. *Chem. Rev.* **1965**, *65*, 635−684.
(34) Bockris, J. O.; Reddy, A. K. N.; Gamboa-Aldeco, M. E. *Modern Electrochemistry 2A: Fundamentals of Electrodics*; Springer: Boston, 2002, DOI: 10.1007/b113922.
(35) Jachimska, B.; Wasilewska, M.; Adamczyk, Z. Characterization of Globular Protein Solutions by Dynamic Light Scattering, Electrophoretic Mobility, and Viscosity Measurements. *Langmuir* **2008**, *24*, 6866−6872.
(36) Agak, J. O.; Stoodley, R.; Retter, U.; Bizzotto, D. On the Impedance of a Lipid-Modified Hg | Electrolyte Interface. *J. Electroanal. Chem.* **2004**, *562*, 135−144.
(37) Hoar, T. P. *Double Layer and Electrode Kinetics*; Interscience Publishers: 1966, *11* (7), 945, DOI: 10.1016/0013-4686(66)87073-1.
(38) Eden, J.; Gascoyne, P. R. C.; Pethig, R. Dielectric and Electrical Properties of Hydrated Bovine Serum Albumin. *J. Chem. Soc., Faraday Trans. 1* **1980**, *76*, 426−434.
(39) Yang, S.; Mirau, P. A.; Pai, C.-S.; Nalamasu, O.; Reichmanis, E.; Pai, J. C.; Obeng, Y. S.; Seputro, J.; Lin, E. K.; Lee, H.-J.; Sun, J.; Gidley, D. W. Nanoporous Ultralow Dielectric Constant Organosilicates Templated by Triblock Copolymers. *Chem. Mater.* **2002**, *14*, 369−374.
(40) Lin, C.-M.; Wu, P.-C.; Lee, M.-J.; Lee, W. Label-Free Protein Quantitation by Dielectric Spectroscopy of Dual-Frequency Liquid Crystal. *Sens. Actuators, B* **2019**, *282*, 158−163.
(41) Li, L.; Li, C.; Zhang, Z.; Alexov, E. On the Dielectric "Constant" of Proteins: Smooth Dielectric Function for Macromolecular Modeling and Its Implementation in DelPhi. *J. Chem. Theory Comput.* **2013**, *9*, 2126−2136.
(42) Green, R. J.; Tasker, S.; Davies, J.; Davies, M. C.; Roberts, C. J.; Tendler, S. J. B. Adsorption of PEO-PPO-PEO Triblock Copolymers at the Solid/Liquid Interface: A Surface Plasmon Resonance Study. *Langmuir* **1997**, *13*, 6510−6515.
(43) Bartlett, P. N. *Bioelectrochemistry: Fundamentals, Experimental Techniques and Applications*; Bartlett, P. N., Ed.; John Wiley & Sons: Chichester, UK, 2008, DOI: 10.1002/9780470753842.
(44) Bravo-Anaya, L. M.; Macías, E. R.; Hernández-López, J. L.; Fernández-Escamilla, V. V.; Carreon-Alvarez, A.; Rodríguez, J. R.; Soltero, J. F. A.; Larios-Durán, E. R. Structural Behavior of Au-Calf Thymus DNA Interface Estimated Through an Electrochemical Impedance Spectroscopy and Surface Plasmon Resonance Study. *Electrochim. Acta* **2014**, *131*, 60−70.
(45) Anson, F. C. Patterns of Ionic and Molecular Adsorption at Electrodes. *Acc. Chem. Res.* **1975**, *8*, 400−407.
(46) Ferapontova, E. E. Electrochemistry of Guanine and 8-Oxoguanine at Gold Electrodes. *Electrochim. Acta* **2004**, *49*, 1751−1759.
(47) Álvarez-Ramírez, J. G.; Fernández, V. V. A.; Macías, E. R.; Rharbi, Y.; Taboada, P.; Gámez-Corrales, R.; Puig, J. E.; Soltero, J. F. A. Phase Behavior of the Pluronic P103/Water System in the Dilute and Semi-Dilute Regimes. *J. Colloid Interface Sci.* **2009**, *333*, 655−662.
(48) Linse, P. Micellization of Poly(Ethylene Oxide)-Poly(Propylene Oxide) Block Copolymers in Aqueous Solution. *Macromolecules* **1993**, *26*, 4437−4449.
(49) Hoeve, C. A. J. Theory of Polymer Adsorption at Interfaces. *J. Polym. Sci., Part C: Polym. Symp.* **1971**, *34*, 1−10.
(50) Kawaguchi, M.; Takahashi, A. Polymer Adsorption at Solid-Liquid Interfaces. *Adv. Colloid Interface Sci.* **1992**, *37*, 219−317.
(51) Andelman, D.; Joanny, J.-F. Polyelectrolyte Adsorption. *C. R. Acad. Sci., Ser. IV: Phys., Astrophys.* **2000**, *1*, 1153−1162.
(52) Dobrynin, A. V.; Rubinstein, M. Theory of Polyelectrolytes in Solutions and at Surfaces. *Prog. Polym. Sci.* **2005**, 1049−1118.
(53) Silberberg, A. Adsorption of Flexible Macromolecules. IV. Effect of Solvent-Solute Interactions, Solute Concentration, and Molecular Weight. *J. Chem. Phys.* **1968**, *48*, 2835−2851.
(54) Palacio, M.; Schricker, S.; Bhushan, B. Morphology and Protein Adsorption Characteristics of Block Copolymer Surfaces. *J. Microsc.* **2010**, *240*, 239−248.
(55) Liu, D.; Wang, T.; Keddie, J. L. Protein Nanopatterning on Self-Organized Poly(Styrene-b-Isoprene) Thin Film Templates. *Langmuir* **2009**, *25*, 4526−4534.
(56) Chang, D.; Lam, C. N.; Tang, S.; Olsen, B. D. Effect of Polymer Chemistry on Globular Protein-Polymer Block Copolymer Self-Assembly. *Polym. Chem.* **2014**, *5*, 4884−4895.
(57) Lin, T.-Y.; Hu, C.-H.; Chou, T.-C. Determination of Albumin Concentration by MIP-QCM Sensor. *Biosens. Bioelectron.* **2004**, *20*, 75−81.

https://dx.doi.org/10.1021/acsomega.0c01704
ACS Omega 2020, 5, 17347−17355